13th International Conference on
Structural Health Monitoring of Intelligent Infrastructure
DOI: 10.3217/978-3-99161-057-1-023

AI-driven Smart-Liner System with DFOS for Digital Twin-Based Real-Time Monitoring of Oil and Gas Infrastructure

Junyi Duan[1], Xingyu Wang[2], Huaixiao Yan[1], Sike Wang[1], Ying Huang[2], Chengcheng Tao[1*]
[1]School of Construction Management Technology, Purdue University, West Lafayette, Indiana 47907, USA
[2]Department of Civil, Construction, and Environmental Engineering, North Dakota State University, Fargo, North Dakota 58102, USA
Email: duan102@purdue.edu, xingyu.wang@ndsu.edu, yan486@purdue.edu, wang6711@purdue.edu, ying.huang@ndsu.edu, tao133@purdue.edu

ABSTRACT: This study presents an innovative AI-powered smart-liner system designed to enhance the safety and efficiency of oil and gas transportation and storage infrastructure. By integrating polymer composite liners with distributed fiber optic sensors (DFOS), the system enables continuous monitoring of mechanical deformations and damage formation, providing real-time insights into the infrastructure's condition throughout its lifespan. Finite element analysis (FEA) is employed to simulate the mechanical responses of the smart-liner-protected specimen over time. Machine learning (ML) algorithms are applied to analyze images generated from collected DFOS data, enabling the identification and assessment of risk variations across different locations and time steps. This approach demonstrates the high accuracy and effectiveness of ML in automatically detecting deformations and crack formation under buckling loading conditions. The methods enable comprehensive structural health monitoring, allowing for precise localization, visualization, and quantification of mechanical changes and damage within the infrastructure. With the above approaches, the smart-liner system facilitates continuous data collection across the entire protected surface, supporting the development of a dynamic digital twin model that evolves alongside the infrastructure. The findings provide critical insights for the oil and gas industry, offering an advanced and efficient solution for monitoring and mitigating risks associated with transportation and storage infrastructure.

KEY WORDS: Distributed fiber optic sensors; Structural health monitoring; Finite element analysis; Machine learning.

1 INTRODUCTION

As the traditionally most energy-consuming industry in the United States [1], the oil and gas industry relies on an extensive network of pipelines, storage tanks, and processing facilities to transport and store hydrocarbons. The infrastructure network is crucial for maintaining the stability and efficiency of the energy supply chain, ensuring that the country can meet its growing energy demands and support rapid economic growth. However, pipeline infrastructure is subjected to various mechanical, environmental, and operational stresses that can lead to material degradation, structural deformations, and eventual failures. Such failures pose significant risks, including environmental pollution, financial losses, and safety hazards for personnel and surrounding communities. A notable example of oil and gas infrastructure failure is the Deepwater Horizon oil spill in the Gulf of Mexico, which occurred in 2010. This disaster is one of the largest and most devastating oil spills in history. The primary cause was the failure of the cement and shoe track barriers, allowing the uncontrolled surge of high-pressure hydrocarbons to escape from the wellbore, travel up the riser, and ignite the oil spillage [2]. Additionally, the San Bruno pipeline explosion occurred in the same year due to the fracture in the welded seam, resulting in the eight deaths [3]. These catastrophic events show significant needs for protecting and monitoring the health conditions of the oil and gas infrastructure.

Ensuring the mechanical resilience of infrastructure is crucial. One way to protect the oil and gas infrastructure is by implementing a polymer composite liner, which is made of fiber fabric and polymer composite. It serves as an additional protective layer, protecting metallic pipelines and storage tanks from mechanical stress, corrosion, and environmental degradation [4], [5]. Polymer composite liners provide significant advantages, including high strength-to-weight ratios, corrosion resistance, and enhanced durability [6]. The liners are engineered to withstand extreme environmental conditions, making them ideal for high-risk applications such as oil and gas transportation and storage. However, despite these benefits, the liner-protected infrastructure still faces structural challenges. One critical issue is mechanical deformation, which can occur due to factors such as thermal expansion, pressure fluctuations, external impacts, and ground movement. Over time, these deformations may lead to localized buckle or collapse, ultimately compromising the structural integrity [7]. Traditional monitoring techniques, such as periodic visual inspections and ultrasonic testing, are often insufficient in detecting infrastructure early-stage damage, as many deformations occur beneath the surface or in hard-to-reach areas. Additionally, the liner is always installed on the interior surface of infrastructure, making the inspection and maintenance even more difficult. To address these limitations, a practical and efficient structural health monitoring (SHM) system is necessary to ensure prolonged service of liner-protected oil and gas infrastructure.

Distributed fiber optic sensor (DFOS) is widely used in monitoring structural health, for its ability of continuous measurement along the fiber length [8]. DFOS operates by transmitting light pulses through optical fibers and analyzing the backscattered signals to measure strain and temperature along the fiber length. This capability is particularly important for large-scale infrastructure, where traditional sensors are impractical or insufficient. Besides, DFOS has advantages in

DOI: 10.3217/978-3-99161-057-1-023

small size, lightweight, water resistance, and suitable for harsh working environments such as extreme weather conditions and seismic-prone regions, making it applicable and reliable in the oil and gas industry [9]–[11]. Zhang et al. [12] attached DFOS on the exterior surface of the pipeline to monitor its compressive and tensile strain distribution. Inaudi and Glisic [13] monitored the conditions of gas pipelines with DFOS for two years. The measured strain and temperature results showed high accuracy. The installation method of both DFOS and liner involves attaching them to the interior surface of the target object. Therefore, the integration of DFOS and polymer composite liner is worth exploring, as it has the potential for simultaneous structural protection and real-time SHM. The DFOS-embedded liner system becomes "smart", which facilitates continuously track of strain variations, and provides early warnings before critical failure occurs. For example, with the continuous measurement and sensitivity properties of DFOS, it is widely applied to detect cracks in concrete structures [14]. Thus, it also has the potential to detect cracks in liners for the development of a comprehensive SHM for oil and gas infrastructure. This integration marks a significant advancement in SHM, enabling a proactive approach to oil and gas infrastructure maintenance.

With the development of smart sensor and AI technology, digital twin becomes an emerging technology in civil and infrastructure applications. DFOS is a critical component in a digital twin model, for its capacity of collecting and updating real-time data [15]. Digital twin model acts as a dynamic, real-time, virtual representation of physical structures. It continuously evolves based on data and simulators for real-time monitoring purpose [16]. Although DFOS provides real-time strain monitoring data, the digital twin model has limitations in presenting the structural shape, for example, the deformation information. To address this issue, finite element analysis (FEA) is an alternative solution, for its capacity in simulating structural mechanical responses efficiently. As the infrastructure is monitored using DFOS, real-time strain data can be correlated to FEA simulation results to find the corresponding deformation information, which supports the development of the digital twin model. The correlation approach requires a high-efficiency method to satisfy the requirement of real-time monitoring purpose. Hence, the AI-driven machine learning (ML) based method is proposed to automatically identify the most accurately correlated pairs. Then the structural deformation is reconstructed and provided to establish an efficient, real-time digital twin model in a rapid response time. Additionally, minor damages are found in the polymer composite liners of oil and gas pipelines [17]. The early detection and maintenance are vital for structural safety. By integrating DFOS with FEA and AI-driven correlation methods, an efficient and real-time digital twin model can be developed to enhance structural health monitoring. This approach not only improves real-time visualization of structural behavior but also facilitates early damage detection, ultimately contributing to the safety and longevity of critical oil and gas infrastructure.

In this paper, we develop a smart-liner system with DFOS to protect and real-time monitor the strain responses of oil and gas infrastructure. FEA and AI-driven approaches are paired with the smart sensor data to identify the digital twin-based real-time SHM function. Section 2 introduces the experimental design, including the materials used to prepare the test sample and experimental instrumentation. Section 3 provides the method of DFOS strain field generation and interpolation function for damage identification and localization. Furthermore, the steps for the digital twin model establishment are introduced, including developing the finite element model for experimental validation and conducting AI-driven strain field correlation between DFOS and FEA results. Section 4 presents the strain field comparison results. Meanwhile, the minor damages in the test sample are identified and localized. Afterward, the best correlated strain fields are fed back to FEA for the development of the digital twin model. This study aims to investigate the feasibility of a smart-liner system with DFOS in real-time structural health monitoring of oil and gas infrastructure, and the accuracy of the digital twin model in representing the structural information. By inducing the buckling load, the study has the potential to provide valuable insights into damage identification, localization, and prevention, contributing to the enhanced safety and reliability of oil and gas infrastructure.

2 EXPERIMENTAL DESIGN

2.1 Materials

The materials prepared to develop the smart-liner protected metallic substrate, including metallic substrate, polymer composite liner, DFOS, and adhesive layer. A 152.4 mm × 304.8 mm (W × L) steel plate is used as a substrate, which represents the metallic pipes and vessels that store and transport oil and gas. A commercial Starline® 2000 polymer composite liner made of woven fabric and polyurethane/polyethylene coating serves as a protective layer for the metallic substrate. The installation of DFOS is a critical step in sample preparation. One Luna high-definition DFOS is first firmly attached to the surface of the liner with a thin coating of 3M DP460 epoxy adhesive. After the adhesive is consolidated, the DFOS-installed liner is then securely attached to a metallic substrate through a 1 mm thick epoxy resin adhesive layer, which simulates the liner rehabilitation for oil and gas pipelines. The prepared sample is placed at room temperature for 24 hours to ensure it is fully cured. The installation of DFOS does not require specialized tools or expert personnel, making it suitable for practical field applications where ease of deployment is essential.

The schematic of a smart-liner protected metallic substrate sample is shown in Figure 1. The sample contains three layers: polymer composite liner, adhesive layer, and metallic substrate. The DFOS is embedded into the interface between the liner and adhesive layer. The thicknesses of each layer from top to bottom are 1.94 mm, 1 mm, and 0.81 mm, respectively. The DFOS, though delicate and easily fractured, is flexible which allows for embedment in a semi-circular style for turning installation direction. It is equipped with a thin, sensitive optic fiber inside, and protected by a multi-layer coating. The DFOS used in this study relies on Rayleigh scatting of light. When a laser pulse travels through the fiber, a small portion of the light is scattered in all directions due to its natural inhomogeneities [18]. External loads, such as mechanical stress, thermal expansion, or vibrations, induce strain in the fiber, causing measurable changes in the backscattered Rayleigh signal. By analyzing these changes, the system can detect variations in

DOI: 10.3217/978-3-99161-057-1-023

strain along the length of the fiber. We install a 5 m fiber length long DFOS, covering the strain measurement area in a zig-zag pattern.

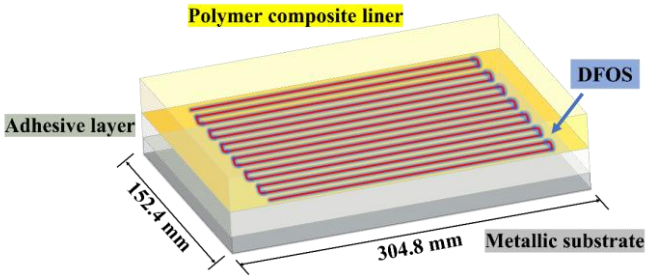

Figure 1. Schematic of a smart-liner protected metallic substrate.

2.2 Experimental instrumentation

To introduce the buckling damage on the smart-liner protected metallic substrate, it is placed in an MTS Criterion® Electromechanical Test Systems, which has a force capacity up to 600 kN. As shown in Figure 2, the sample is clamped on the two edges along the longitudinal direction and subjected to an eccentric buckling load, simulating real-world complex structural deformation. The two clamped sections have same dimension with 25.4 mm × 30 mm (W × L). The loading machine is controlled by a constant displacement rate of 0.2 mm/min, with a total vertical displacement of 5 mm. Luna optical distributed sensor interrogator (ODiSI) 6100 is used for strain data collection from DFOS. When backscattered light interferes with the reference signal in the interrogator, it generates an interference pattern containing phase and amplitude information, which correlates with strain variations along the fiber. By applying a fast Fourier transform, the system extracts high-resolution, spatially continuous strain data. This processed data is used to generate a high-resolution strain profile along the fiber length, providing a real-time, visually accessible strain plot on the ODiSI control platform.

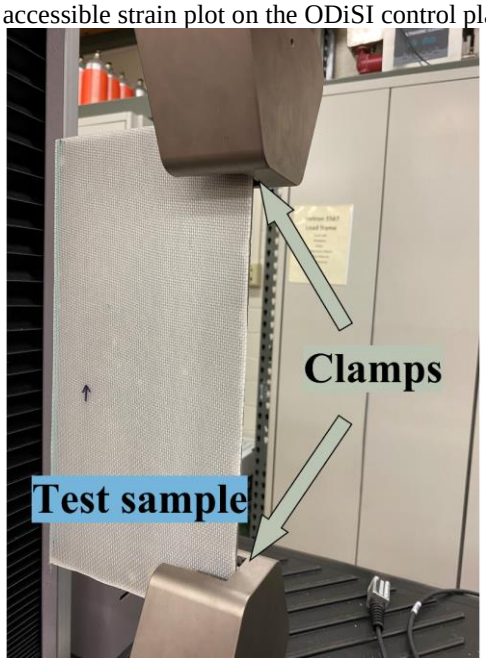

Figure 2. The smart-liner protected metallic substrate sample clamped in loading machine.

3 RESEARCH METHODOLOGY

3.1 DFOS strain field generation

The measurement performance of DFOS is highly reliant on its settings, including measurement rate and gauge pitch. If the measurement rate is too high, the generated strain data not only occupies excessive storage and computational resources but also contains unnecessary noise. Previous DFOS applications in engineering practices used measurement rates ranging from 5 to 50 Hz [19]–[21]. In this study, the measurement rate is set to 10 Hz to balance the measurement accuracy and efficiency. Gauge pitch, also called spatial resolution, refers to the distance between each measurement point along the optic fiber. The measurement area in our case is relatively small, as shown in Figure 2. A large gauge pitch, for example, 5.2 mm [22], is inapplicable. Since this is a laboratory experiment conducted with a short DFOS length, the highest available spatial resolution of 0.65 mm is selected to achieve a dense strain measurement [23].

The illustration of the smart-liner system with DFOS is shown in Figure 3. The DFOS is attached to the polymer composite liner surface in a zig-zag pattern, forming 14 distinct measurement lines with a uniform spacing of 10 mm. L1 represents the first line, and L14 is the last line close to the clamped edge, which is subjected to the largest buckling deformation. The blue stars represent the measurement point along the fiber. As discussed earlier, the distance between two contiguous measurement points equals the gauge pitch of 0.65 mm. DFOS covers an area of 130 mm × 200 mm, for strain monitoring purpose.

The generation of the DFOS strain field contains the conversion of the one-dimensional strain data to the two-dimensional strain field, through the X-Y coordinate system, as shown in Figure 3. For example, to map the strain data point on L1 into the strain field, the Y-coordinate is fixed along the line, and the X-coordinate is uniformly increasing at the rate of gauge pitch. In this approach, the DFOS strain field is generated, enabling visualization representation of strain distribution for smart-liner system.

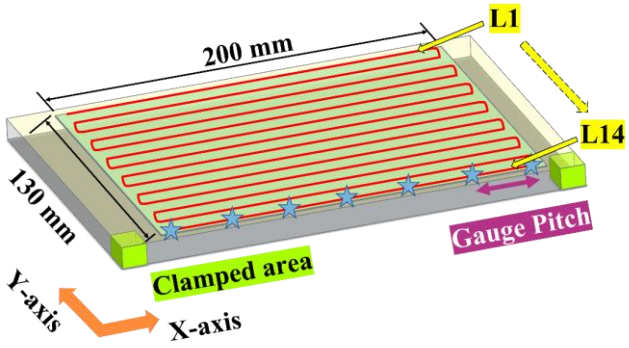

Figure 3. Schematical illustration of the smart-liner system with DFOS.

3.2 Damage identification and localization

To promote the application of DFOS for real-time monitoring of large oil and gas infrastructures, automated damage identification and localization are essential. When the DFOS

DOI: 10.3217/978-3-99161-057-1-023

passes through a crack, a significant increase in strain rate is always detected, making it appliable to identify the presence and location of cracks [24]. To achieve the identification, obtaining strain values on a finer grid is the prerequisite. Bilinear interpolation and triangle-based interpolation are two widely employed planar interpolation algorithms for estimating unknown data based on known data in two-dimensional plane [25]. This study applies bilinear interpolation to estimate the strain on a finer grid, because DFOS has a fixed gauge pitch, the collected strain is uniformly distributed. Bilinear interpolation is a method the uses repeated linear interpolation to interpolate functions of two variables, which typically used on regular grids. Equation (1) illustrates how this method estimates the value for a target point using four neighboring lattice points.

$$f(x,y) \approx w_{11}f(Q_{11}) + w_{12}f(Q_{12}) + w_{21}f(Q_{21}) + w_{22}f(Q_{22}) \quad (1)$$

where (x_1, y_1) , (x_1, y_2) , (x_2, y_1) , (x_2, y_2) are the coordinates of the four neighboring lattice points Q_{11} , Q_{12}, Q_{21}, Q_{22}. The weights w are listed as follows:

$$w_{11} = \frac{(x_2 - x)(y_2 - y)}{(x_2 - x_1)(y_2 - y_1)}$$

$$w_{12} = \frac{(x_2 - x)(y - y_1)}{(x_2 - x_1)(y_2 - y_1)}$$

$$w_{21} = \frac{(x - x_1)(y_2 - y)}{(x_2 - x_1)(y_2 - y_1)}$$

$$w_{22} = \frac{(x - x_1)(y - y_1)}{(x_2 - x_1)(y_2 - y_1)}$$

The gradient calculation formula, shown in Equation (2), represents the slope limit as the distance between two neighboring lattice points d approaches zero. A denser grid provides a gradient closer to the true value but increases computational costs. Based on a convergency study, we determine to interpolate strain value on 0.1 mm × 0.1 mm grid, as further reducing the grid size has little impact on the gradient.

$$\text{gradient} = \lim_{d \to 0} \frac{f(x+d) - f(x)}{d} \quad (2)$$

3.3 Establishment of digital twin model

This study aims to develop a smart-liner system with DFOS to enable digital twin-based real-time monitoring of oil and gas infrastructure. Once the smart-liner system with DFOS collects the real-time, accurate strain results, we establish a digital twin model for virtual and real-time representation. To build the virtual model, we create a three-dimensional finite element model to replicate the experimental testing on smart-liner protected metallic substrate. Section 3.3.1 presents the detailed design, including geometry, interfacial contact, and mesh information, to construct the finite element model to simulate the smart-liner protected metallic substrate under the eccentric buckling load. Section 3.3.2 shows the AI-driven method to correlate the DFOS-measured strain field and FEA-predicted strain field. This method facilitates deformation reconstruction and the digital twin model establishment to visualize buckling deformed smart-liner system in the real-time.

3.3.1 Finite element model design

FEA is carried out to simulate the smart-liner protected metallic substrate under the buckling load, correlate strain results with the experimental study, and generate deformation information to establish the digital twin model. FEA is a powerful computational tool that enables accurate prediction of structural behavior under various loading conditions, which is widely applied in the oil and gas transportation and storage infrastructure [26]. By simulating experimental scenarios, it reduces the need for costly physical samples, saving both time and resources. Abaqus/CAE 2024 is employed to generate and analyze the finite element model in this study. The finite element model has same geometry and material settings as the test sample with three layers: metallic layer, the adhesive layer, and liner layer. To generate the mesh for this thin and multi-layer object, the widely-used C3D8R (8-node linear brick element with reduced integration) element is not the best choice. Instead, we select the C3D8S (8-node linear brick element with improved surface stress visualization) element for discretization, because of its advantage in estimating surface strain [27]. The mesh size of this model is 2.5 mm uniformly. The material properties of each layer are presented in Table 1. The metallic substrate is made of high-ductility steel and simulated using a bilinear model with strain hardening. The adhesive layer and polymer composite line have significantly lower stiffness compared to the metallic substrate. Thus, elastic models are applied in the analysis.

Table 1. Material properties in finite element model.

Layer	Material property
Metallic substrate	Young's modulus = 210 GPa Poisson's ratio = 0.3 Yield strength = 500 MPa Ultimate strength = 635 MPa Ultimate strain = 0.2
Adhesive layer	Young's modulus = 1 GPa Poisson's ratio = 0.3
Polymer composite liner	Young's modulus = 400 MPa Poisson's ratio = 0.4

Figure 4 exhibits the finite element model of the smart-liner protected metallic substrate. The bottom edge areas are constrained to move and rotate, identical to the bottom clamped area in the experiment. The top edge is also constrained to rotation but allowed for a vertical displacement of 5 mm, accurately replicating the experimental buckling load setup. The interfacial contact between two interfaces is simplified as tied, given the careful curing procedures, to simulate a perfectly bonded condition.

DOI: 10.3217/978-3-99161-057-1-023

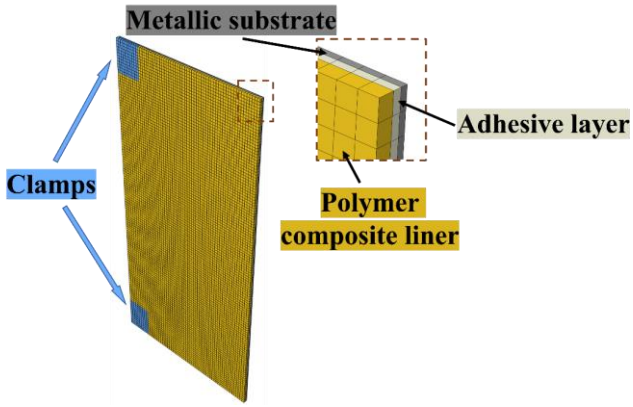

Figure 4. Finite element model of smart-liner protected metallic substrate.

Performing a buckling analysis in Abaqus involves two steps: linear eigenvalue analysis, and nonlinear Riks analysis. The linear eigenvalue analysis is the first step, which estimates the critical buckling load and corresponding mode shape. This method assumes small deformations and linear material behavior, making it computationally efficient. While this method is useful for obtaining a quick estimate of the buckling load, it does not account for geometric imperfections, material nonlinearities, or post-buckling behavior, which may lead to inaccurate predictions. Therefore, we also conduct nonlinear Riks analysis that accounts for geometric and material nonlinearities, as well as initial imperfections. The geometric and material nonlinearities are enabled by changing the setting and inputting material nonlinear properties. The first three mode shapes from linear eigenvalue analysis serve as the initial imperfections. The magnitudes of the first, second, and third buckling mode shapes are set as 1.00%, 0.50%, and 0.25% of the plate thickness, respectively [28]. The predicted strain distribution is compared with the DFOS strain field result for validation purpose, and then correlated with the DFOS strain field to generate corresponding deformation distribution to establish the digital twin model.

3.3.2 AI-driven strain field correlation

It is common for the strain data from experiments and simulations to exhibit slight differences, because of the discreteness of the experiment. To fill this gap, this research implements a strain field correlation method based on the convolution neural network (CNN) to find the most similar pair between DFOS and FEA results. Figure 5 illustrates the basic process of strain field correlation. The inputs are strain field images generated from DFOS and FEA, from which CNN can be used to extract the abstract features. Then, the cosine similarity between the extracted features of the DFOS and FEA data is compared. Through iterating over the entire FEA database, the best matching pair is found. In order to enhance the feature-extracting capability of CNN, the pre-trained ResNet18 model is used to process the input images. ResNet is a classic CNN that has shown extraordinary feature extraction ability in engineering fields [29], [30]. We employ ResNet18, one of the smallest models of ResNet, to process images, and its output feature maps are flattened to a one-dimensional vector for comparison. The best matching pair will be fed back into FEA for deformation generation and digital twin model establishment.

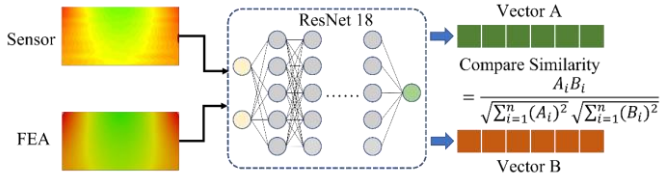

Figure 5. The workflow of strain field correlation.

4 RESULTS AND DISCUSSION

4.1 Strain field comparison between experiment and FEA

The one-dimensional DFOS data collected on the interface between the adhesive layer and polymer composite liner is converted to a two-dimensional strain field for visualization and comparison, following the methodology introduced in Section 3.3.2. The strain results with the increasing vertical displacement levels are shown in Figure 6. The positive strain in the middle of the right edge is represented in yellow, indicating the tensile strain. The negative strain at the corners of the right edges is represented in dark blue showing the compressive strain. The strain fields show an approximately symmetric pattern with respect to the central transverse line. As the test sample is subjected to an eccentric load and clamped at the corners of the left edges symmetrically, resulting in a symmetric strain distribution. The slight asymmetry can be attributed to the instrumental limitations such as the minor drifts.

Additionally, the strain distribution contours on the interface between the adhesive layer and liner are obtained from FEA results, as shown in Figure 6. To facilitate the comparison, the strain fields from DFOS and FEA are extracted at the same displacement level and share the same colormap. Due to the advantage of numerical analysis is free of external disturbances, the comparison results show that FEA has a symmetric strain distribution, which is highly similar to the results from DFOS. For further validation, we apply pixel-based comparison to quantify the similarity between DFOS and FEA results, by using the parameters including structural similarity index measure (SSIM) and mean absolute percentage error (MAPE). Table 2 presents the strain field comparison results. The SSIM results for the three cases are approximately around 0.9, indicating the results from DFOS and FEA have high similarities. MAPE results provide the relative error percentage between DFOS and FEA results, which demonstrate that the difference is less than 0.60%. Overall, the strain comparison demonstrates that the FEA results have good agreement with the DFOS results, validating the accuracy of the finite element model. Building on this, FEA can help DFOS expand the capacity from strain monitoring to mechanical performance monitoring, reconstruct the structural deformation, and facilitate the establishment of the digital twin model.

DOI: 10.3217/978-3-99161-057-1-023

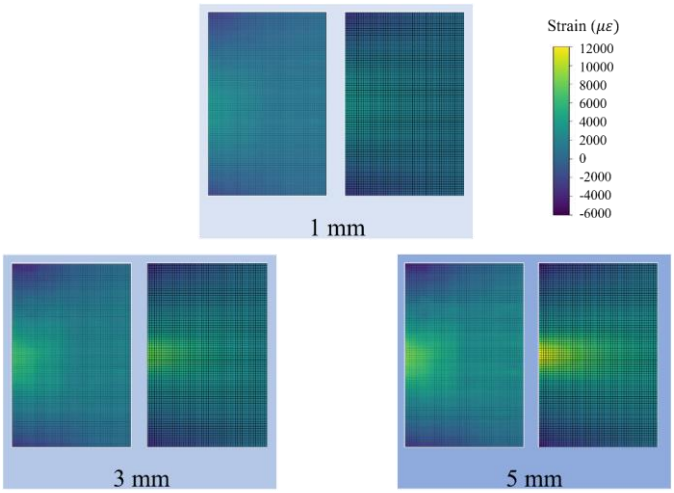

Figure 6. Strain distribution fields with increasing vertical displacements collected from DFOS (left), and FEA (right).

Table 2. Strain field comparison results.

Displacement level	SSIM	MAPE
1 mm	0.91	0.56%
3 mm	0.91	0.22%
5 mm	0.89	0.60%

4.2 Identification and localization of potential damages in adhesive layer

The identification of potential damages is important, as they often correspond to the areas where failure initiates. The damages on the adhesive layer are hard to detect visually so a non-destructive monitoring method is necessary. As introduced in Section 3.2, the DFOS strain rate has a significant increase when it passes a crack. By converting the location of the strain rate surge into two-dimensional coordinates, we can localize the damage in the structure, which enables real-time structural damage monitoring. After processing the strain data from DFOS using interpolation and gradient calculation, we can visualize the region where the strain rate increases rapidly. Figure 7 shows the plot of strain gradient distribution. We set the strain gradient limit of damage as 200, any region with a strain gradient greater than 200 is highlighted in red circles. The results show that damages commonly occur close to the edge, near the highest strain region. It is also observed that, although the strain field distribution has a symmetric pattern, the potential damage has not. Therefore, the identification and localization of damage becomes more significant, as they are unpredictable. This method leverages the continuous measurement capacity of DFOS, enabling the detection and mapping of the potential damage. It enhances the efficiency of real-time structural damage monitoring, can be employed to identify potential damages in liner-rehabilitated oil and gas infrastructure, and extends the structural service life.

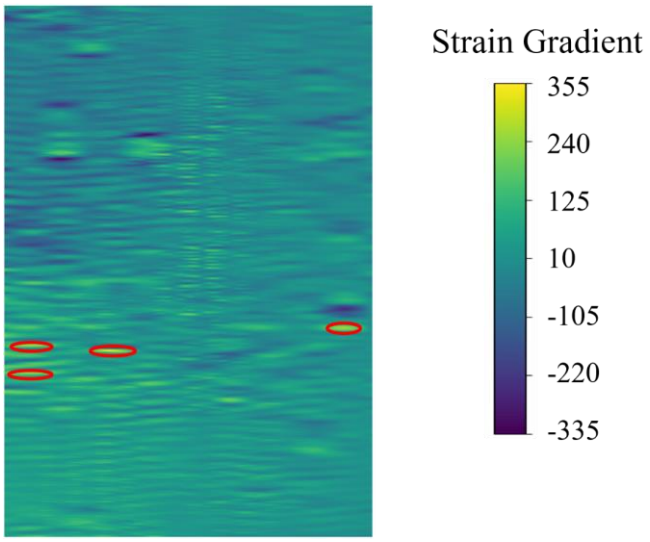

Figure 7. The location of potential damages in adhesive layer.

4.3 Strain correlation and digital-twin model establishment of buckled liner-protected metallic substrate

Although DFOS and FEA results demonstrated a good agreement, the strain field correlation is required for an accurate representation of deformation reconstruction. In terms of the strain field correlation methods as introduced in Section 3.3.2, the DFOS strain fields at 1 mm, 3 mm, and 5 mm displacement levels are inputted into the AI-driven strain correlation model and set as ground truth. FEA strain fields are organized as a database, which includes all FEA strain fields at every 0.01 mm displacement. By extracting the features from DFOS strain fields and iteratively comparing the cosine similarities of the FEA strain field database, the most similar pairs are found. Table 3 shows the strain correlation results. We compare the corresponding displacements of the correlated strain field pairs. It can be seen that the correlation results have some differences, but the difference is not significant, remaining within an acceptable millimeter-level range for practical applications in the oil and gas industry.

Based on strain correlation results, we reconstruct the deformation and establish the digital twin model of the buckled liner-protected metallic substrate, as illustrated in Figure 8. The digital twin model presents the key deformation characteristics and provides a predictive framework for real-time monitoring. The comparison and correlation between the experimental and numerical strain fields verify the effectiveness of the digital twin model. The digital twin framework enables continuous tracking of deformation states, which is crucial for real-time SHM, enabling dynamic, real-time, virtual representation of the liner-protected metallic substrate. This study highlights the potential of a smart-liner system with DFOS in combination with a digital twin model for structural integrity assessment. The findings support the feasibility of using digital twin models for predictive maintenance and damage prevention in oil and gas infrastructure. Although the implementation of the digital twin model faces challenges, such as high initial investment and potential incompatibility, experimental investigation demonstrates its capability for real-time monitoring of liner-protected substrate conditions, with the potential to prevent even greater financial losses resulting from pipe failure. Additionally, the installation of CIPP liners is a mature and

DOI: 10.3217/978-3-99161-057-1-023

widely adopted practice. The integration method developed in this study also confirms the durability of DFOS under buckling conditions. Therefore, the implementation of the smart-liner system is both feasible and promising for practical applications.

Table 3. Strain field correlation results.

Displacement level	Correlated displacement	Difference
1 mm	0.81 mm	-0.19 mm
3 mm	3.38 mm	+0.38 mm
5 mm	4.75 mm	-0.25 mm

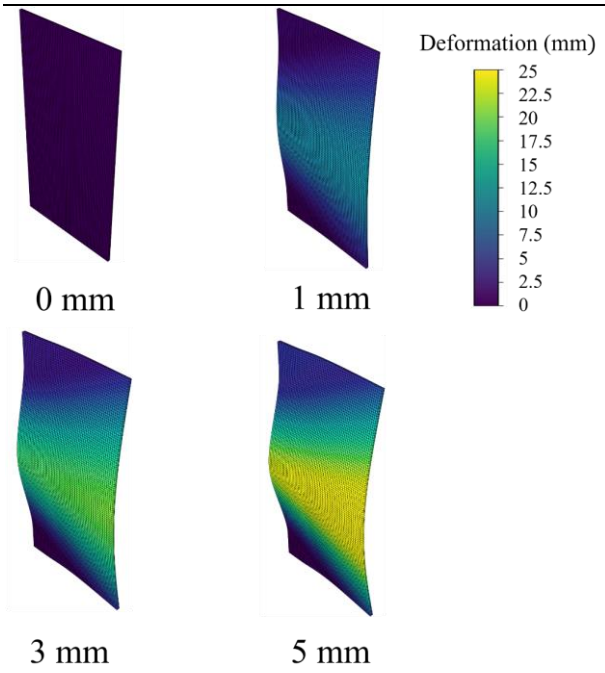

Figure 8. Digital twin model of buckled liner-protected metallic substrate with increasing deformation.

5 CONCLUSION

In this paper, we establish a digital twin-based real-time monitoring system for oil and gas infrastructure by integrating smart sensor technology, finite element analysis, and deep learning algorithms. Through the embedment of the distributed fiber optic sensor into the polymer composite liner, this study validates the feasibility and accuracy of the smart-liner system in real-time monitoring of the strain fields, without compensating the protective capability of the liner. Enhanced by finite element analysis, the smart-liner system achieves the capability from strain monitoring to structural mechanical performance monitoring. Further improved with a deep learning-based approach, the digital-twin model is generated for visualization of a three-dimensional smart-liner protected substrate with accurate deformation representation. In addition to the external visualization, some flaws inside of the structure, such as cracks, are be detected through the smart-liner system, showing the robust health monitoring capabilities. Several summarized conclusions are listed as follows:

- The durability of DFOS under large deformation is promising. Under an extreme buckling scenario, as shown in this study, the DFOS can constantly provide accurate and continuous data, and facilitate strain field monitoring for oil and gas infrastructure.
- The finite element analysis results are of high accuracy, with a lowest SSIM of 0.89, and highest MAPE of 0.60% compared to experimental results. This validates the reliability of developed finite element model in predicting structural behavior, supporting its use in generating digital twin model.
- The smart-liner system has the capacity to identify and localize minor cracks in the adhesive layer with high efficiency, realizing early maintenance and rehabilitation.
- The AI-driven strain correlation analysis establishes a foundation for developing the digital twin model. This model provides a real-time, three-dimensional representation of the structural physical conditions, enabling accurate structural health monitoring for oil and gas infrastructure.

In summary, this study proposes a framework for establishing the digital twin model for real-time structural health monitoring of oil and gas infrastructure. This study has limitations in assessing the proposed framework on the smart-liner protected metallic substrate. Scaling this study to large and complex oil and gas transportation and storage infrastructure networks introduces challenges such as data management, sensor deployment, and integration with existing large-scale infrastructure. With the advancement of high-performance computing technologies, data analytics is becoming increasingly capable of handling the vast amount of information generated by distributed sensing systems. Distributed sensing technologies have already been applied in large-scale structures such as bridges, railways, and pipelines [31], [32], demonstrating their feasibility and robustness in extensive monitoring applications. Furthermore, the widespread application of polymer composite liners in the oil and gas industry supports the practical applicability of scaling up the developed smart-liner system for structural health monitoring across extensive networks of pipelines and storage facilities. Future work will be expanded to the long-term durability test, aiming to investigate the long-term performance of smart-liner system and digital-twin models.

ACKNOWLEDGMENTS

The authors express their gratitude to the funding provided to support this study from USDOT PHMSA through Grant Number 693JK32250009CAAP, an Early-Career Research Fellowship from the Gulf Research Program of the National Academies of Sciences, Engineering, and Medicine through Grant Number SCON-10000955, and the American Chemical Society Petroleum Research Fund through Grant Number PRF # 67005-DNI9. The findings and opinions expressed in this article are those of the authors only and do not necessarily reflect the views of the sponsors.

REFERENCES

[1] M. C. Guilford et al., ‘A new long term assessment of energy return on investment (EROI) for US oil and gas discovery and production’, *Sustainability*, vol. 3, no. 10, pp. 1866–1887, 2011.

[2] M. Bly, *Deepwater Horizon accident investigation report*. Diane Publishing, 2011.

DOI: 10.3217/978-3-99161-057-1-023

[3] R. M. Peekema, 'Causes of Natural Gas Pipeline Explosive Ruptures', *J. Pipeline Syst. Eng. Pract.*, vol. 4, no. 1, pp. 74–80, 2013.
[4] L. C. Hollaway, 'Using fibre-reinforced polymer (FRP) composites to rehabilitate differing types of metallic infrastructure', in *Rehabilitation of Metallic Civil Infrastructure Using Fiber Reinforced Polymer (FRP) Composites*, Elsevier, 2014, pp. 323–372.
[5] V. Motaharinejad et al., 'Enhancement of adhesion between the polymeric liner and the metallic connector of high-pressure hydrogen storage tank', *Int. J. Mater. Form.*, vol. 14, no. 2, pp. 249–260, 2021.
[6] M. A. Karim et al., 'An assessment of the processing parameters and application of fibre-reinforced polymers (FRPs) in the petroleum and natural gas industries: A review', *Results Eng.*, vol. 18, p. 101091, 2023.
[7] B. Harrison et al., 'Measurement of lined pipe liner imperfections and the effect on wrinkling and collapse under bending', in *International Conference on Offshore Mechanics and Arctic Engineering*, 2016, vol. 49965, p. V005T04A036.
[8] T. Howiacki et al., 'Crack shape coefficient: comparison between different DFOS tools embedded for crack monitoring in concrete', *Sensors*, vol. 23, no. 2, p. 566, 2023.
[9] I. Ashry et al., 'A review of distributed fiber–optic sensing in the oil and gas industry', *J. Light. Technol.*, vol. 40, no. 5, pp. 1407–1431, 2022.
[10] M. C. L. Quinn et al., 'Distributed Fiber Optic Sensing in Cold Regions', in *Geo-Congress 2024*, Vancouver, British Columbia, Canada, 2024, pp. 536–544.
[11] B. Glisic and Y. Yao, 'Fiber optic method for health assessment of pipelines subjected to earthquake-induced ground movement', *Struct. Health Monit.*, vol. 11, no. 6, pp. 696–711, 2012.
[12] S. Zhang et al., 'Pipeline deformation monitoring using distributed fiber optical sensor', *Measurement*, vol. 133, pp. 208–213, 2019.
[13] D. Inaudi and B. Glisic, 'Long-range pipeline monitoring by distributed fiber optic sensing', 2010.
[14] M. Herbers et al., 'Crack monitoring on concrete structures: Comparison of various distributed fiber optic sensors with digital image correlation method', *Struct. Concr.*, vol. 24, no. 5, pp. 6123–6140, 2023.
[15] M. F. Bado et al., 'Digital twin for civil engineering systems: An exploratory review for distributed sensing updating', *Sensors*, vol. 22, no. 9, p. 3168, 2022.
[16] A. Rasheed et al., 'Digital twin: Values, challenges and enablers from a modeling perspective', *IEEE Access*, vol. 8, pp. 21980–22012, 2020.
[17] H. U. Khalid et al., 'Permeation Damage of Polymer Liner in Oil and Gas Pipelines: A Review', *Polymers*, vol. 12, no. 10, p. 2307, 2020.
[18] K. Sharma et al., 'A System Design Perspective for Measurement of Parameters Using Different Scatterings Associated with Fibre Optic Sensors', in *Proceedings of Third International Conference on Communication, Computing and Electronics Systems*, vol. 844, Singapore: Springer Singapore, 2022, pp. 793–813.
[19] L. Meng et al., 'A research on low modulus distributed fiber optical sensor for pavement material strain monitoring', *Sensors*, vol. 17, no. 10, p. 2386, 2017.
[20] C. G. Berrocal et al., 'Crack monitoring in reinforced concrete beams by distributed optical fiber sensors', *Struct. Infrastruct. Eng.*, vol. 17, no. 1, pp. 124–139, 2021.
[21] L. Fan et al., 'Feasibility of distributed fiber optic sensor for corrosion monitoring of steel bars in reinforced concrete', *Sensors*, vol. 18, no. 11, p. 3722, 2018.
[22] Y. Tang et al., 'Structural and sensing performance of RC beams strengthened with prestressed near-surface mounted self-sensing basalt FRP bar', *Compos. Struct.*, vol. 259, p. 113474, 2021.
[23] M. Herbers et al., 'Rayleigh-based crack monitoring with distributed fiber optic sensors: experimental study on the interaction of spatial resolution and sensor type', *J. Civ. Struct. Health Monit.*, 2024.
[24] X. Tan and Y. Bao, 'Measuring crack width using a distributed fiber optic sensor based on optical frequency domain reflectometry', *Measurement*, vol. 172, p. 108945, 2021.
[25] I. Amidror, 'Scattered data interpolation methods for electronic imaging systems: a survey', *J. Electron. Imaging*, vol. 11, no. 2, pp. 157–176, 2002.
[26] P. Jukes et al., 'The latest developments in the design and simulation of deepwater subsea oil and gas pipelines using FEA', in *ISOPE International Deep-Ocean Technology Symposium*, 2009, p. ISOPE-D.
[27] C. Colombo et al., 'Numerical investigation of wire-clamp contact for a drawing machine', *Procedia Struct. Integr.*, vol. 24, pp. 225–232, 2019.
[28] E. L. Liu and M. A. Wadee, 'Mode interaction in perfect and imperfect thin-walled I-section struts susceptible to global buckling about the strong axis', *Thin-Walled Struct.*, vol. 106, pp. 228–243, 2016.
[29] T. S. Prajwal and I. A K, 'A Comparative Study Of RESNET-Pretrained Models For Computer Vision', in *Proceedings of the 2023 Fifteenth International Conference on Contemporary Computing*, Noida India, 2023, pp. 419–425.
[30] W. Xu et al., 'ResNet and its application to medical image processing: Research progress and challenges', *Comput. Methods Programs Biomed.*, vol. 240, p. 107660, 2023.
[31] J. Xu et al., 'Full scale strain monitoring of a suspension bridge using high performance distributed fiber optic sensors', *Meas. Sci. Technol.*, vol. 27, no. 12, p. 124017, 2016.
[32] K. Soga and L. Luo, 'Distributed fiber optics sensors for civil engineering infrastructure sensing', *J. Struct. Integr. Maint.*, vol. 3, no. 1, pp. 1–21, 2018.